

Co-delivering of RNase A-NBC and Glucose Oxidase for Targeted
Cancer Therapy

A thesis submitted by

Jingqiong Xu

in partial fulfillment of the requirement for the degree of

Master of Science

in

Biomedical Engineering

TUFTS UNIVERSITY

August 2015

Adviser: Qiaobing Xu, Ph.D.

Abstract

Using chemotherapeutic protein in cancer treatment has been increasingly researched as it provides advantages over traditional therapeutics in both safety and efficacy. However, the current commonly-used chemotherapeutic proteins and protein delivery methods have many limitations, calling for innovative protein-based formulations delivered by novel methods. Previously, Dr. Qiaobing Xu's lab has demonstrated the utility of lipidoid nanoparticles for intracellular protein delivery. The successful delivery of RNase A, a potential cancer chemotherapeutic protein, modified with a reactive oxygen species (ROS) responsive modification (RNase A-NBC) to tumor cells, showed cancer specific induced cytotoxicity. However, this delivery scheme could be further improved by co-delivery with another chemotherapeutic protein. Here, we propose a novel combination formulation comprised of Glucose Oxidase (GOx), a ROS-generating protein, and RNase A-NBC delivered using lipidoid nanoparticles. The feasibility and optimization of this combination formulation was first evaluated based on the toxicity of each protein independently delivered to HeLa tumor cells. Subsequently, the lipidoid co-delivery of proteins was evaluated and optimized. Successful intracellular delivery using this combination formulation induced cytotoxicity in the HeLa tumor cell line. In addition, the combination formulation demonstrated a synergistic drug effect as it induced a higher death rate of HeLa cells than the arithmetic sum of GOx or RNase A-NBC alone. Finally, the glucose dependence of the cytotoxicity was also demonstrated by GLUT inhibition experiments. These results suggest a strong potential for this GOx & RNase A-NBC

combination formulation to be applied in future cancer treatment, and the bright future for lipidoid nanoparticles to be used in protein based drug deliveries.

Acknowledgements

First and foremost, I would like to thank my advisor Dr. Qiaobing Xu, for all of his guidance and insights over the past two years. I would also like to thank my committee members, Dr. Lauren Black and Dr. Ayse Asatekin, for their continuous encouragement.

Moreover, I would like to thank all members in Xu Lab. Special thanks to Dr. Ming Wang, for his endless support. I would also like to thank all members in the Biomedical Engineering Department at Tufts. Special thanks to Martin Hunter and Ying Chen, for their help with operating the experimental equipment.

Last but not the least, I would like to thank my family for their love and support in my desire to pursue a M.S. degree in Biomedical Engineering at Tufts.

Table of Contents

CHAPTER 1. INTRODUCTION	1
1.1 Cancer and glucose metabolism.....	1
1.1.1 Background on Cancer.....	1
1.1.2 Glucose metabolism in cancer cells	2
1.1.3 Glucose transporters (GLUT)	3
1.1.4 Glucose transport inhibitors.....	5
1.1.5 Glucose oxidase (GOx)	6
1.2 Reactive Oxygen Species (ROS)-responsive protein modification for cancer therapy	9
1.2.1 RNase and Cancer therapy	9
1.2.2 The reactive oxygen species in cancer cells.....	10
1.2.3 The ROS and RNase A-NBC system	12
1.3 Protein therapeutics delivery by lipids nanoparticles	14
1.3.1 Drug delivery for protein therapeutics.....	14
1.3.2 EC16-80 lipidoid nanoparticles.....	15
CHAPTER 2. STUDY OF THE RNASE ACTIVITY OF RNASE A-NBC WITH THE INFLUENCE OF GOX AND GLUCOSE.....	18
2.1 Materials and Methods	18
2.1.1 Preparation of Stock RNase A-NBC Solution	18
2.1.2 RNase A Activity Assay	19
2.2 Results and Discussion	20
2.2.1 Protein Concentration Assay	20
2.2.2 RNase A Activity Assay	21
CHAPTER 3. SYNERGISTIC EFFECT STUDY OF ROS-RESPONSIVE PROTEIN AND GOX DELIVERED BY THE CATIONIC LIPID-LIKE NANOPARTICLES	24
3.1 Materials and Methods	24
3.1.1 Materials	24
3.1.2 Culture of HeLa Cells	24
3.1.3 <i>In Vitro</i> Cytotoxicity Assay Set-up	24
3.1.4 Cytotoxicity Study of the Cationic Lipid-like Nanoparticles EC16-80 Dependent on the Concentration	25

3.1.5 EC16-80/RNase A-NBC Nanoparticles Delivery	25
3.1.6 EC16-80/GOx Nanoparticles Delivery	26
3.1.7 Synergistic Effect of Protein Combination Delivery	26
3.1.8 Thiazolyl Blue Tetrazolium Bromide (MTT) Assay	27
3.2 Results and Discussion	28
3.2.1 Cytotoxicity of the Cationic Lipid-like Nanoparticles EC16-80 Dependent on the Protein Concentration	28
3.2.2 Cytotoxicity resulted from EC16-80/RNase A-NBC Nanoparticles Delivery	29
3.2.3 Cytotoxicity resulted from EC16-80/GOx Nanoparticles Delivery	31
3.2.4 Synergistic Effect of Protein Combination Delivery on HeLa cells	33
CHAPTER 4. STUDY OF GLUCOSE DEPENDENCE OF COMBINATION FORMULATION.....	35
4.1 Materials and Methods	35
4.1.1 Materials	35
4.1.2 Increased Glucose Culture Treatment before Protein Combination Delivery	35
4.1.3 No Glucose Culture Treatment before Protein Combination Delivery	35
4.1.4 Inhibition of GLUT Activity Treatment before Protein Combination Delivery	36
4.2 Results and Discussion	36
4.2.1 Results of Increased Glucose Culture Treatment for Protein Combination Delivery ..	36
4.2.2 Results of No Glucose Culture Treatment for Protein Combination Delivery	37
4.2.3 Inhibition of GLUT Activity Treatment for Protein Combination Delivery	39
CHAPTER 5. CONCLUSIONS.....	40
REFERENCE.....	41

List of Tables

Table 2.1 Preparation of Diluted Albumin (BSA) Standards	18
Table 2.2 RNase A Activity Assay of combination formulations.....	20
Table 3.1 Combination Formulations of GOx, RNase A-NBC and EC16-80.....	27

List of Figures

Figure 1.1 Glucose oxidation and subsequent reactions.....	7
Figure 1.2 RNase A modification, delivery and restoration.....	13
Figure 1.3 Scheme for lipidoid nanoparticles.	16
Figure 2.1 Absorbance (562nm) curve for BSA standards and sample measurement.....	21
Figure 2.2 RNase A activity assay of RNase A-NBC with a variety of GOx and Glucose combinations.	22
Figure 3.1 The cell viability assay to determine the cytotoxic concentration of EC16-80 lipidoid.	28
Figure 3.2 Cell viability assay to determine the association of RNase A – NBC concentration and cytotoxicity.....	30
Figure 3.3 Cell viability assay to determine the association of RNase A – NBC concentration and cytotoxicity at the presence of EC16-80.	31
Figure 3.4 Cell viability assay to determine association of the cytotoxicity of GOx and its dose. 32	
Figure 3.5 Cell viability assay to determine association of the cytotoxicity of GOx and its dose with the presence of EC16-80 at 150 ng / 10,000 cells.	33
Figure 3.6 The viability of HeLa cells across different drug delivery groups.	34
Figure 4.1 The viability of HeLa cells across different drug delivery groups, after double glucose culture for the day previous to study.	37
Figure 4.2 The viability of HeLa cells across different drug delivery groups, after glucose starvation for the day previous to study.	38
Figure 4.3 The viability of HeLa cells across different drug delivery groups, after phloretin treatment to inhibit the GLUTs and thus the intracellular transport of glucose.	39

CHAPTER 1. INTRODUCTION

1.1 Cancer and glucose metabolism

1.1.1 Background on Cancer

Cancer is one of the major diseases that cause human deaths. As estimated by WHO World Cancer Report 2014, there are about 14.1 million new cases of cancer and about 8.2 million deaths caused by cancer in 2012. Cancer is characterized by the rapid proliferation of abnormal cells and impairment of death mechanisms in the affected cells. As a result, extra abnormal cells will generate and form tumors. Many cancers form solid tumors, which are masses of tissue. One exception is leukemia, which does not form solid tumors. At later stages of cancer, the abnormal cells can undergo metastasis, which means to spread from their initial site by local spread, lymphatic spread or blood to nearby locations, regional lymph nodes or distant sites. As a consequence, other organs of the body may be invaded and damaged, causing failure of the organ and even lethal effect to the subject.

It was estimated that 90–95% of cancer cases are due to environmental factors, which includes radiation, obesity, tobacco, infections, stress and environmental pollutants. The remaining 5–10% are due to inherited genetics (Anand et al. 2008). Nevertheless, genomic instability are observed in all cancer cells. Some genes that regulate cellular mechanisms could be altered to

permit the rapid growth of cells and impair cell death program. When cancer occurs, two categories of genes are usually altered: the oncogenes and tumor suppressor genes. The former can promote cell growth and proliferation while the latter usually inhibit cell reproduction and survival. Therefore the formation of oncogenes or over-expression of normally expressed oncogenes, and the loss or under-expression of tumor suppressor genes may both lead to the transformation of normal cell into cancer cells (Croce 2008) .

With the instability in cancer cell genomics, cancer cells acquire multiple biological capabilities during the development of cancer. These capabilities include excessive proliferative signaling, insensitivity to growth suppression signaling, cell death resistance, replicative immortality and metastasis transformation. In addition, tumor can escape from immune destruction to preserve itself as well as trigger angiogenesis and reprogram energy metabolism to support its rapid growth and proliferation (Hanahan and Weinberg 2011).

1.1.2 Glucose metabolism in cancer cells

Cellular energy metabolism alteration is one of the hallmarks indicating the transition from normal to cancer cells. Glycolysis is an energy-producing metabolic process that converts one molecule of glucose to two pyruvates with the production of two ATP and two reduced nicotinamide adenine dinucleotide (NADH) molecules. With oxygen, pyruvate can be oxidized to CO₂ and H₂O via the oxidative phosphorylation pathway, finally generating 36 molecules of ATP. On the other hand, without oxygen pyruvate can be transformed into lactic acid via the

anaerobic glycolysis pathway. In some cases, aerobic glycolysis (also known as Warburg effect), which is the conversion of glucose to lactic acid in the presence of oxygen, can also occur (Warburg 1956). This is true for most cancer cells, which produce large amounts of lactate regardless of the presence of oxygen. Currently it is still unclear which mechanisms trigger aerobic glycolysis in cancer cells. It was assumed that hypoxia, which is the usual situation before angiogenesis occurs, drives tumor cells onto the aerobic glycolysis pathway. However, evidence also showed glycolytic switch is acquired very early in carcinogenesis even before tumors experience hypoxia (Vander Heiden et al. 2009). Regardless of the triggering mechanism, aerobic glycolysis clearly provides the cancer cells advantages in tumor development, such as higher resistance to apoptosis and abilities of rapid growth and invasive spread. At the same time, aerobic glycolysis can be a potential target for novel anticancer therapies (Annibaldi and Widmann 2010).

1.1.3 Glucose transporters (GLUT)

The transport of glucose across the plasma membrane into the cytosol is mediated by a family of glucose transporters (GLUTs) (Medina and Owen 2002). GLUTs control the movement of glucose between intracellular and extracellular compartments to ensure the cell obtains constant glucose for metabolism (Augustin 2010). The transport of glucose by GLUTs belongs to facilitated diffusion, which is an ATP-independent and bi-directional transportation of glucose across the cell membrane down the concentration gradient. Since the glucose transport process is a rate-limiting step in glucose metabolism, to support its requirement for large amounts of

energy, cancer cell abnormally up-regulate the GLUTs to ensure the increased uptake of glucose (Adekola et al. 2012).

The genes of the GLUT family belong to the 2A solute carrier family. So far there have been 14 isoforms of the GLUT genes discovered and grouped into three classes based on their primary sequences. Class I is known as the classical transporters and comprises GLUT 1–4 as well as GLUT 14, which is considered to be a gene duplicate of GLUT 3. Class II is made up of GLUT 5, 7, 9 and 11, whereas class III is composed of GLUT 6, 8, 10, 12 and 13 (Macheda et al. 2005).

Class I GLUTs are the first discovered and most characterized for their expression, function in glucose transport and roles in carcinogenesis. GLUT 1, which is normally expressed in erythrocytes, placenta, and endothelial cells, has been found to be overexpressed in a variety of cancers, including B-cell lymphoma, colorectal carcinomas, prostate carcinoma, thyroid carcinoma, renal cell cancer, lung cancer, pancreatic cancer and laryngeal carcinomas (Jun et al. 2011, Grabellus et al. 2012). GLUT 2 has the lowest affinity for glucose among GLUTs family. It has been expressed in the cancer cell lines of the small intestine, kidney, breast, insulinoma, colon and pancreas. GLUT 3 has been found to be expressed predominantly in the brain and also tissues that demands high level of glucose, such as the placenta and testes (Augustin 2010). GLUT 3 has been investigated in cancer cell lines including choriocarcinoma , retinoblastoma, breast, ovarian and colorectal cancers (Medina and Owen 2002). GLUT 4, which is normally found in insulin-sensitive tissue such as cardiac, skeletal and muscular tissue, also demonstrates an important role in sustaining multiple myeloma cell viability and proliferation

(McBrayer et al. 2012). Among the class I GLUTs, it was reported that for HeLa cell lines only expression of GLUT1 and GLUT2 were present on relatively high levels whereas the GLUT3 and GLUT4 signaling were only detected, at best, at negligible levels (Rodriguez-Enriquez et al. 2009).

In contrast to the high specificity for glucose shown in class I GLUTs, other GLUT isoforms seem to prefer other carbohydrates and metabolites (Joost and Thorens 2001). Members in the class II GLUTs are characterized for their ability to transport fructose (Medina and Owen 2002). Similar to the class III GLUTs, their role in cancer is less clear. Some evidence also suggests some members of the GLUTs in class II and III may also play important roles in tumorigenesis. For instance, GLUT 5 has been found to be overexpressed in some types of cancer, such as renal cell carcinoma (RCC), breast and prostate cancer (Medina Villaamil et al. 2011, Wuest et al. 2011, Reinicke et al. 2012)

1.1.4 Glucose transport inhibitors

There are multiple substances that have been shown to be able to specifically inhibit the GLUT activity. For instance, STF-31, which belongs to the second class in the group of compounds pyridyl anilino thiazoles, is able to inhibit glucose uptake and utilization. It was reported STF-31 was cytotoxic in RCC expressing GLUT1 and its cytotoxic effects can be reversed by the expression of high amounts of GLUT2 (Chan et al. 2011). Another GLUT inhibitor is Genistein, which is a naturally occurring isoflavone compound. It shows direct competitive inhibitory

effect on GLUT1, resulting in inhibition of the transport of hexoses and dehydroascorbic acid across the plasma cell membrane (Vera et al. 1996). In addition, fasentin, which is a compound that can sensitize cell to FAS-induced death, was also reported to be able to bind directly to GLUT1 and inhibit glucose uptake of prostate cancer cells and U-937 leukemia cells (Wood et al. 2008).

In our experiment, phloretin was used to inhibit the activity of GLUTs. Phloretin belongs to dihydrochalcones, a type of natural phenols that can be found in fruit trees. It is able to inhibit the active transport of glucose into cells by Sodium/glucose cotransporters including SGLT1 and SGLT2 (Chan and Lotspeich 1962). It is also able to inhibit the facilitated diffusion by GLUTs and, thereby, has been used as a specific inhibitor of GLUT1 (Afzal et al. 2002) as well as GLUT2 (Walker et al. 2005). Phloretin functions as a GLUT inhibitor by binding to the external surface of GLUTs (Krupka 1985). Phloretin has been shown to inhibit the growth of the rat mammary adenocarcinoma and Fischer bladder cell carcinoma cell lines (Nelson and Falk 1993), and also shown *in vitro* to induce the apoptosis of cancer cells by suppressing the glucose transport (Kobori et al. 1997).

1.1.5 Glucose oxidase (GOx)

Glucose oxidase (GOx) can be found in certain species of fungi and insects, such as *Aspergillus Niger*. It is a homodimer made up of two identical 80-kDa subunits and two non-covalently bound flavin adenine dinucleotides (FAD). The FAD coenzyme acts as an electron carrier during

catalysis of glucose at the active site which is in a deep pocket (Wilson and Turner 1992). GOx is able to catalyze the oxidation of beta-D-glucose to produce D-gluconolactone and hydrogen peroxide. Both hydrogen peroxide and D-gluconolactone breaks down spontaneously and catalytically (Figure 1.1).

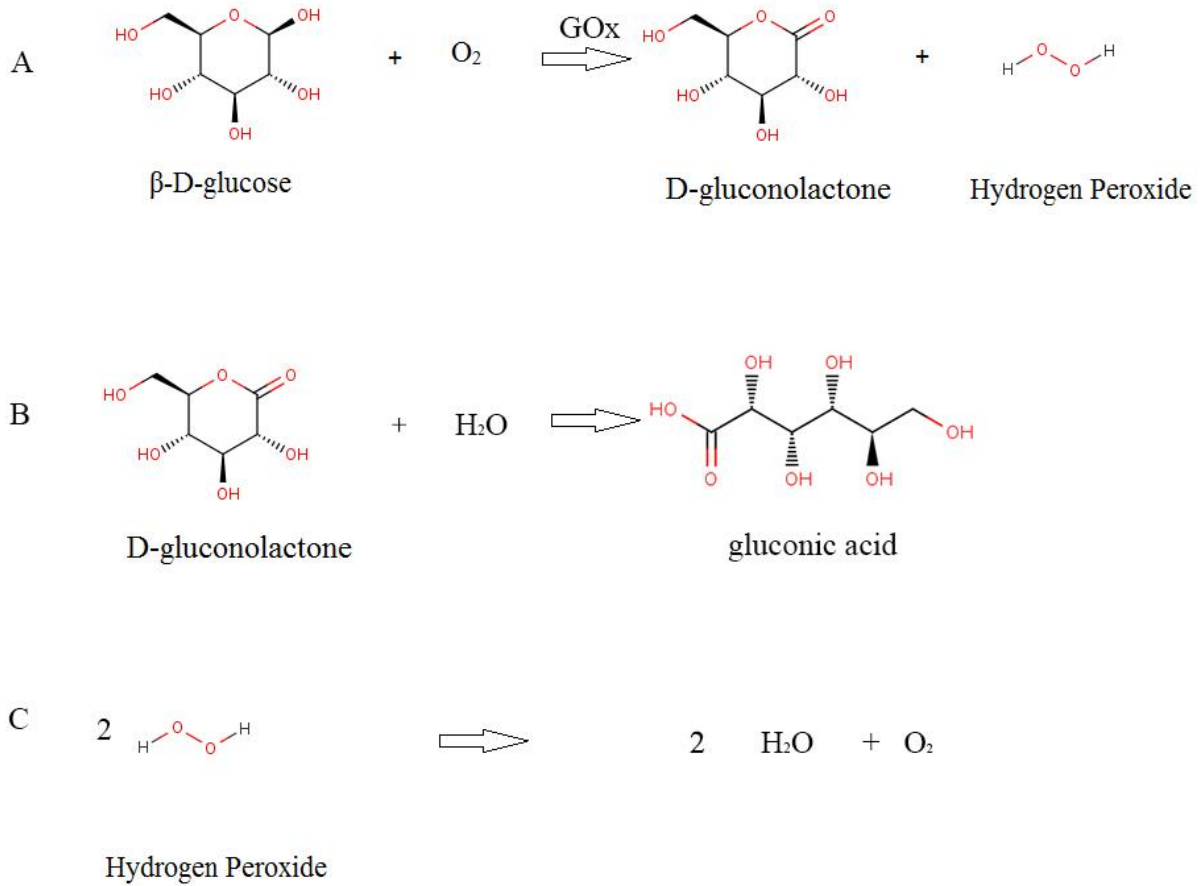


Figure 1.1 Glucose oxidation and subsequent reactions. A: GOx catalyze beta-D-glucose to produce D-gluconolactone and hydrogen peroxide; B: D-gluconolactone can spontaneously or by catalysis produce gluconic acid; C: hydrogen peroxide, which is also the product of glucose oxidation, can be broken down into water and oxygen.

The enzymatic activity of GOx can be regulated by feedback effect, as it is reduced when hydrogen peroxide accumulates and then inactivates the enzyme (Kleppe 1966, Bao et al. 2003). The accumulation of product from D-gluconolactone breakdown, gluconic acid, can also reduce pH of the solution and result in the product inhibition of GOx (Miron et al. 2004).

Besides glucose, glucose oxidase is capable of oxidising other monosaccharides, nitroalkanes and hydroxyl compounds (Wilson and Turner 1992). However, its activity on other substrates are relatively low compared to that on glucose. Those can be oxidized at a significant rate by glucose oxidase from *Aspergillus Niger* includes 6-deoxy-D-glucose (10%) 4-O-methyl-D-glucose (15%) 2-deoxy-D-glucose (20–30%) if using the reaction rate on glucose as the 100% reference. The activities of glucose oxidase on other substrates are usually poor, typically under 2% of its activity on glucose (Pazur and Kleppe 1964, Leskovac et al. 2005).

Since its discovery, GOx has been widely used in many industry fields, including food processing, bread making, food preservation, reduced alcohol wine production and even fuel cell and textile industry (Wong et al. 2008). Researchers are also investigating extensively innovative application of GOx in the biomedical field, for instance, to treat cancer and other diseases.

1.2 Reactive Oxygen Species (ROS)-responsive protein modification for cancer therapy

1.2.1 RNase and Cancer therapy

RNase A was first discovered in bovine pancreas, by which it was named as bovine pancreatic ribonuclease A. Since its discovery, it has been well characterized and used as a model system for biochemists for many different types of experiments, both as an enzyme and as a well-characterized protein for biophysical studies (Marshall et al. 2008). Compared to other members in its family (RNase B, C & D), RNase A does not undergo glycosylation modification (Plummer and Hirs 1963). RNase A is small protein composed of a single chain polypeptide containing four disulfide bridges. Its mature form has only 124 amino acid residues and 13.7 kDa molecular mass. It also has excellent heat and detergent stability. Due to the above properties, RNase A has become a target of synthetic chemists since long time ago and was the first protein to succumb to total synthesis (Merrifield 1985). As an endoribonuclease, RNase A attacks at the 3' phosphate of a pyrimidine nucleotide, resulting in the sequence of pG-pG-pC-pA-pG cleaved to give pG-pG-pCp and A-pG (Raines 1998).

Due to the ability of cleaving RNA and thus rendering the genetic information of the cell indecipherable, some homologues of RNase A has been reported to induce cytotoxic effects when taken up by cells (Saxena et al. 1991, Leland et al. 1998). For instance, ranpirinase isolated from the oocytes of the Northern leopard frog show differential cytotoxicity against tumor cells *in vitro* and *in vivo* dependent on its catalytic activity (Lee and Raines 2008, Ardelt et al. 1991).

RNase A therapies have been investigated in clinical trials as an alternative protein therapeutic approach for treating cancer patients besides traditional methods including surgery, radiation therapy, and chemotherapy (Lee and Raines 2008).

1.2.2 The reactive oxygen species in cancer cells

By definition, the reactive oxygen species (ROS) are oxygen-containing chemical species with reactive chemical properties. ROS include free radicals such as superoxide and hydroxyl radicals, which contain an unpaired electron, and non-radical molecules such hydrogen peroxide (H_2O_2) (Pelicano et al. 2004). In normal cells, ROS are generated through various pathways constantly, involving both enzyme-catalyzed reaction and spontaneous reaction. The most important organelles for ROS production is mitochondria. During the oxidative phosphorylation in mitochondria, electrons are transmitted through the electron transport chain (ETC), finally establishing a proton gradient across the inner mitochondrial membrane to drive ATP synthesis. During this process, superoxide can be produced as some electrons may escape from the ETC, especially from complexes I and III, and react with molecular oxygen to form superoxide (Saybasili et al. 2001, Staniek et al. 2002). It was reported that about 2% of the oxygen consumption within the mitochondria will form superoxide, which is finally converted to hydrogen peroxide (Boveris and Chance 1973, Fridovich 1995)

Compared to normal cells, many types of tumor cells and tissues have elevated levels of ROS which may be contributed by several mechanisms. First, oncogenic signals may increase ROS

generation. For instance, besides its ability to induce DNA damage and p53 deactivation, the oncogene c-myc can also increase ROS generation (Vafa et al. 2002). Similarly, the oncogenic RAS2 allele can cause the sustained activation of cAMP-PKA pathway, which can also increase ROS production and, therefore, oxidative protein damage (Hlavata et al. 2003).

The second mechanism may be the malfunction of the mitochondrial respiratory chain. The mitochondrial DNA (mtDNA) codes for thirteen components of the ETC. Mutations of mtDNA, which is actually more vulnerable than nuclear DNA, can lead to dysfunctions of ETC components and malfunction of the mitochondrial respiratory chain (Copeland et al. 2002, Kang and Hamasaki 2003). As the mitochondrial respiratory chain is the major site of ROS generation, malfunction of the mitochondrial respiratory chain can result in more free radical production due to increased electrons escaped from the respiratory complex (Pelicano et al. 2004). This situation can be exacerbated by the high demand by cancer cells for high level of ATP supply to maintain rapid cell growth and proliferation. The high stress on the mitochondrial ETC can further contribute to increased ROS generation.

Some other mechanisms may also account for the increased ROS level in cancer cells. For example, certain cancers cause inflammatory responses and promote the generation of ROS (Azad et al. 2008). It was also reported that in certain cancer cells, a decrease in the expression or the activity of antioxidant enzymes, such as SOD, may also impair the ability of cells to eliminate superoxide radicals and cause ROS accumulation in these cells (Van Driel et al. 1997).

1.2.3 The ROS and RNase A-NBC system

Researchers have targeted elevated ROS levels in cancer cells as a basis for developing novel therapies for cancer treatment (Broaders et al. 2011, de Gracia Lux et al. 2012, Shim and Xia 2013). Previously in our lab, we also successfully modified RNase A and developed an innovative method to kill cancer cells by taking advantage of their high cellular level of ROS (Wang, Sun, et al. 2014).

In our approach, RNase A first was modified with 4-nitrophenyl 4- (4,4,5,5-tetramethyl-1,3,2-dioxaborolan-2-yl) benzyl carbonate (NBC). After the reaction, the lysine residue of RNase A, which is essential for its RNase activity, was conjugated with an aryl boronic ester through a covalent carbamate linker (Figure 1.2 B). In The conjugated boronate ester is unstable and quickly hydrolyzed into aryl boronic acid (Achilli et al. 2013), producing boronic acid modified RNase A (RNase A–NBC).

The modified RNase A was then delivered into cancer cells by using synthetic cationic lipid-like nanoparticles. The conjugation of RNase A with aryl boronic acid can decrease the isoelectric point of RNase A. This delivery system enhances intracellular delivery by potentiating its electrostatic interactions with positively charged lipid nanoparticles (Figure 1.2 B). After entering cancer cells, RNase A–NBC was released from the nanoparticles and reactivated by intracellular hydrogen peroxide, which triggers a self-immolative reaction of NBC conjugation, releasing the lysine on RNase A and restoring its activity (Figure 1.2 A) (Broaders et al. 2011).

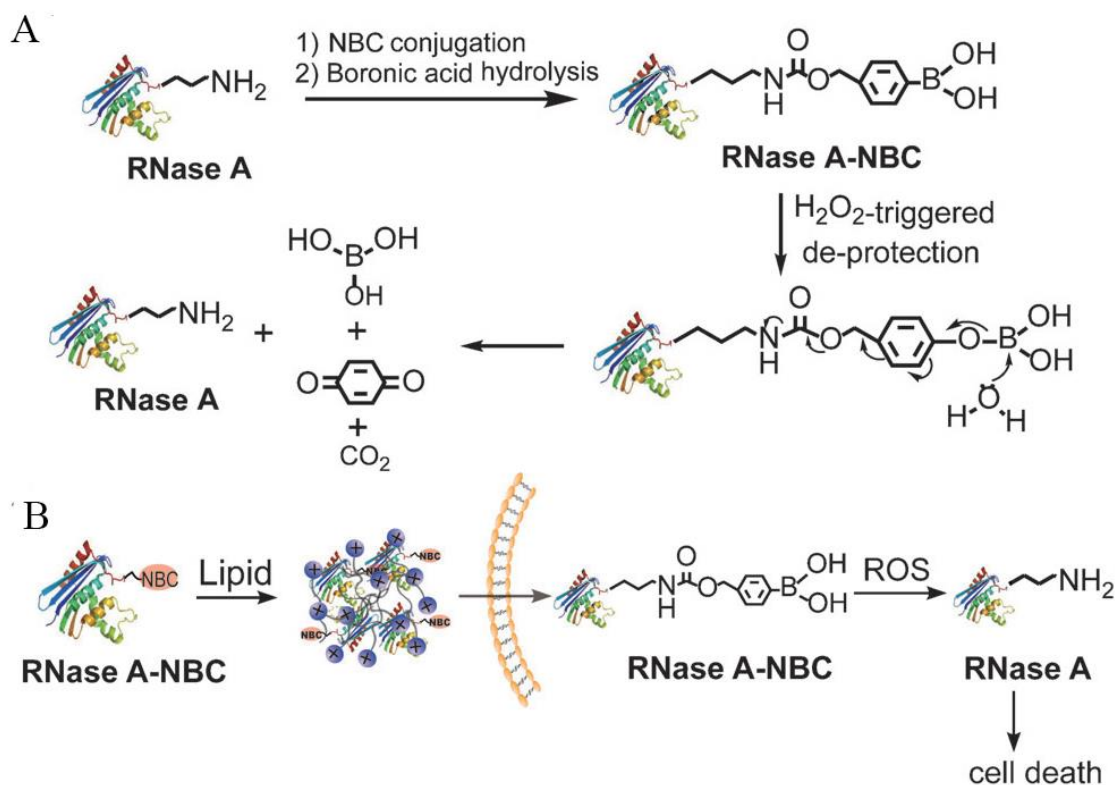


Figure 1.2 RNase A modification, delivery and restoration. A: The modification of RNase and self-immolative reaction trigger by hydrogen peroxide; B: The delivery of RNase-A-NBC by lipidoid nanoparticles (Wang, Sun, et al. 2014).

Our lab demonstrated that the delivery of RNase A-NBC selectively prohibited cancer cell growth by triggering the cytotoxicity of RNase A in cancer cells while remaining nontoxic for normal cells. Our results suggested that by using this system, normal cells could tolerate increased dosage of RNase A, and the efficacy of the system can be further promoted by improving complexation with lipid nanoparticles and, thereby, the efficiency of drug delivery. This indicated the promising prospect of this lipid nanoparticle encapsulated RNase A –NBC system for cancer therapy and further improvement could be done in the future.

1.3 Protein therapeutics delivery by lipids nanoparticles

1.3.1 Drug delivery for protein therapeutics

Since the early 1980s, protein therapies have been developing rapidly as they were considered as the safest and most direct approach for human disease treatment. A majority of protein pharmaceuticals accomplish their therapeutic goal by targeting cell surface ligands or extracellular domains and thus manipulate the cellular functions (Leader et al. 2008). However, many protein pharmaceuticals need to exert their functions by interacting with targets inside the cell. In the latter case, low permeability of cell membranes to macromolecules often positions an additional obstacle for the development of peptide-based and protein-based drug formulations. Therefore, guaranteeing the protein pharmaceuticals are safely and efficiently delivered across the plasma membrane is key for successful protein therapies and remains a challenge that many biomedical researchers are striving to overcome (Torchilin 2009).

Over the past few decades, one of the best studied protein delivery approaches has been fusing target protein cargos with protein transduction domains or membrane transport signals. This approach has the advantage of non-invasiveness and ability for systematic application, compared with traditional methods such as electroporation or microinjection, which can damage the cell and is inappropriate for *in vivo* application. The delivery efficiency of protein transduction domain fusion method varies with protein type. This method also lacks the

capability to target a specific tissue or organ (Mi et al. 2000). In addition, high cost of these methods is also an obstacle preventing it from being applied widely.

Recent years have witnessed unprecedented growth of research and applications in the area of nanoscience and nanotechnology. At the same time, drug delivery systems utilizing nanoparticles have been developing rapidly in recent years, offering alternative approaches for spatially and temporally controlled protein delivery. A number of synthetic nanomaterials, including liposomes (Kim et al. 2012), polymers (Lee and Feijen 2012), and inorganic nanoparticles (Ghosh et al. 2010), have been designed for intracellular protein delivery.

Nevertheless, the nanoparticles based on these materials are still facing problems including the low delivery efficiency, potential unspecific delivery and complex nanoparticle fabrication.

Thus, it is still an urgent task to develop novel nanoparticles to ensure efficient and convenient intracellular protein delivery.

1.3.2 EC16-80 lipidoid nanoparticles

In recent years, the cationic lipid-like materials, which is also named lipidoids, have been generated for siRNA delivery utilizing the combinatorial library strategy (Akinc et al. 2008, Alabi et al. 2013). Previously in our lab, we established a novel and efficient protein delivery platform that uses combinatorially designed cationic lipid based nanoparticles combined with reversible protein modifications. Furthermore, this new delivery approach was also successfully applied in DNA and mRNA intracellular delivery (Wang et al. 2012, Sun et al. 2012). Subsequently, we

successfully proved that the lipidoid nanoparticles can also be utilized as a novel protein delivery platform, as the electric and hydrophobic interactions between lipidoids and proteins can load proteins into lipidoid nanoparticles, whose hydrophobic nature in turn facilitates the transport of cargo protein through the cell membrane. We also demonstrated that by modifying protein by treating the protein with selected chemicals, we could strengthen the charge-charge binding between proteins and lipidoids, and thereby promote the delivery efficiency. The modification can also be reversed in the intracellular environment, resulting in the restoration of the biological activity of protein therapeutics (Wang, Alberti, et al. 2014).

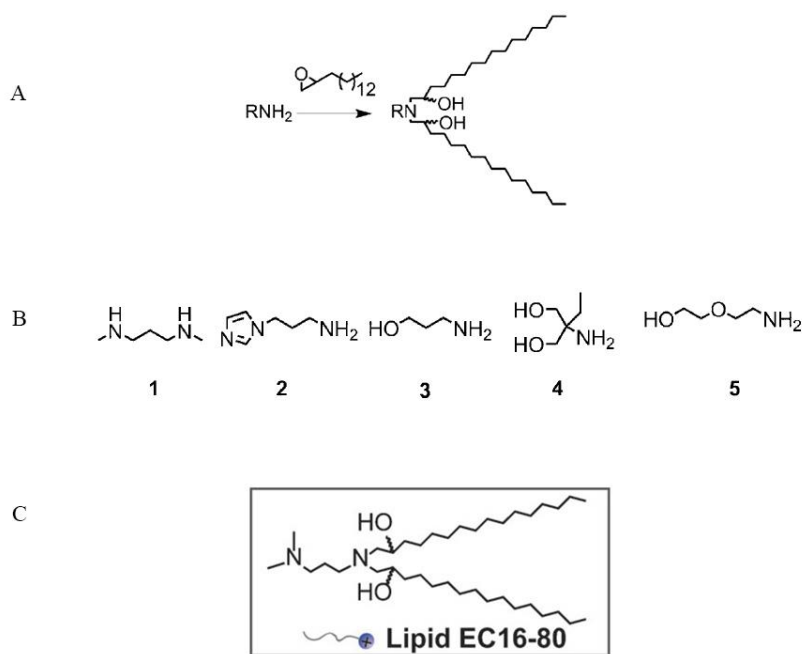


Figure 1.3 Scheme for lipidoid nanoparticles. A: the scheme demonstrating synthesis of lipidoids; B: Some examples in the library of amines used for lipidoid synthesis (EC16-1 to EC16-5) ; C: the structure of lipid EC16-80 (Wang, Alberti, et al. 2014)

The library of lipidoids can be synthesized through the ring opening reaction between 1,2 epoxyhexadecane and amine under mild conditions (Figure 1.3) (Wang et al. 2012). The lipidoids are named EC16 followed by the amine number in the library where EC16 indicates 1,2-epoxyhexadecane. In the research included in this thesis, EC16-80 was utilized to produce the highest efficiency.

CHAPTER 2. STUDY OF THE RNASE ACTIVITY OF RNASE A-NBC WITH THE INFLUENCE OF GOX AND GLUCOSE

2.1 Materials and Methods

The modified protein, RNase A-NBC, was prepared utilizing the method described in previous report (Wang, Sun, et al. 2014). Pierce® BCA Protein Assay Kit was purchased from Thermo Fisher Scientific (Waltham, MA). RNaseAlert® Substrate was purchased from Integrated DNA Technologies (Coralville, Iowa). All other chemicals were purchased from Sigma-Aldrich (St. Louis, MO).

2.1.1 Preparation of Stock RNase A-NBC Solution

Table 2.1 Preparation of Diluted Albumin (BSA) Standards

Vial	Volume of Diluent (μL)	Volume and Source of BSA (μL)	Final BSA Concentration (μg/μL)
A	0	300 of Stock	2000
B	125	327 of Stock	1500
C	325	325 of Stock	1000
D	175	175 of vial B dilution	750
E	325	325 of vial C dilution	500
F	325	325 of vial E dilution	250
G	325	325 of vial F dilution	125
H	400	100 of vial G dilution	25
I	400	0	0

The concentration of RNase A-NBC was assayed using Pierce® BCA Protein Assay Kit. The contents of one Albumin Standard (BSA) ampule were first diluted to prepare a set of protein standards (working range = 20 - 2000 µg/mL) (Table 2.1). The BCA Working Reagent (WR) was prepared by mixing 50 parts of BCA Reagent A with 1 part of BCA Reagent B. After adding 25 µL of each standard or RNase A-NBC sample into a 96 well microplate, 200 µL of the WR was added to each well and mixed thoroughly. The plate was incubated at 37°C for 30 minutes and cooled to room temperature after incubation, then read for absorbance at 562 nm. The absorbance of protein standards was recorded and graphed into a standard curve, which was then compared with the absorbance of RNase A-NBC to determine its concentration.

After calculating the concentration of initial modified protein, the stock RNase A-NBC solution was prepared to be 1 mg/mL by adding NaOAc buffer.

2.1.2 RNase A Activity Assay

The activity of RNase A was assayed using RNaseAlert® Substrate. One tube of bulk substrate was dissolved in 1.0 mL RNase-Free distilled water and mixed well to make the substrate concentration 2 µM. The test group and control were prepared as the Table 2.2 by 1 mg/mL RNase A-NBC, 1 mg/mL GOx and 1 mg/mL Glucose, 1 mg/mL RNase A and incubated at 37°C for 1 h.

Subsequently, 10 µL of RNaseAlert® substrate and 10 µL of 10X RNaseAlert® Buffer were added

to each well of 96 well black plates. After that, 80 μL test or control was added to each well as the Table 2.1 and mixed thoroughly. The plate was read immediately in a fluorimeter for 20 min at 490 nm excitation and 520 nm emission in real time to obtain quantitative kinetic curves.

Table 2.2 RNase A Activity Assay of combination formulations

Group	Treatment (Final volume: 80 μL , by adding RNase-Free water)
Control 1	1 μL RNase A-NBC
Control 2	1 μL GOx
Control 3	1 μL Glucose
Control 4	1 μL RNase A-NBC + 1 μL GOx
Control 5	1 μL RNase A-NBC + 1 μL Glucose
Control 6	1 μL GOx + 1 μL Glucose
Test Group	1 μL RNase A-NBC + 1 μL GOx + 1 μL Glucose
Negative Control	1 μL stock RNase A
Positive Control	Nuclease-Free water

2.2 Results and Discussion

2.2.1 Protein Concentration Assay

The standard curve of BSA is shown as Figure 2.1. As expected, the absorbance of protein solution increase as the concentration elevates. The figure shows an almost linear standard curve and the sample absorbance read is within the linear range, both meeting with the assumption of BCA protein assay. The absorbance of modified protein, RNase A-NBC, is 0.5967,

which stands for 1.131 mg/mL based on the standard curve. To make 1mg/mL stock solution, RNase A-NBC per 1 mL is added 0.131 mL NaOAc buffer.

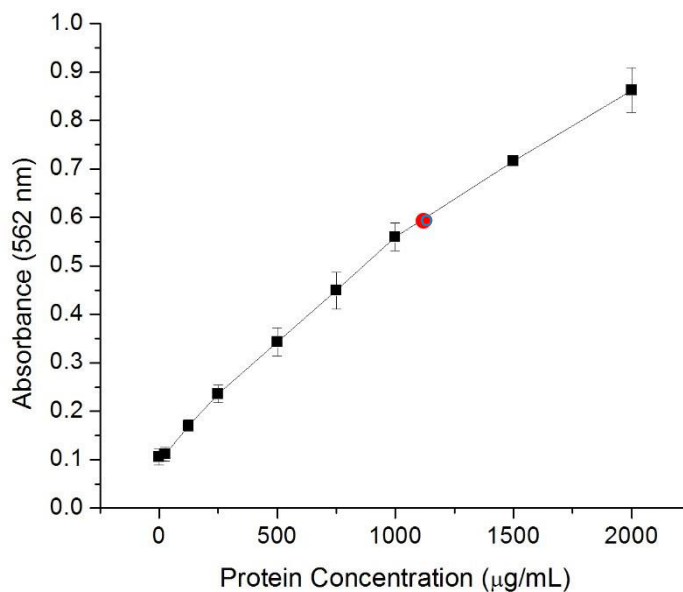


Figure 2.1 Absorbance (562nm) curve for BSA standards and sample measurement. Black dots: measurements for protein standards; Red dot: measurement for RNase-NBC sample.

2.2.2 RNase A Activity Assay

To confirm the feasibility for this GOx & RNase-NBC system, an RNase activity *in vitro* study was first conducted to determine whether RNase A could restore its function in the assumed cellular environment. The RNaseAlert® assay uses RNA substrate tagged with a fluorescent reporter molecule (fluor) on one end and a quencher on the other. In the absence of RNases, the physical proximity of the quencher dampens fluorescence from the fluor to extremely low levels. When RNases activity are present, the RNA substrate is cleaved and the fluor and

quencher are spatially separated in solution. This causes the fluor to emit a bright green signal when excited by light of the appropriate wavelength.

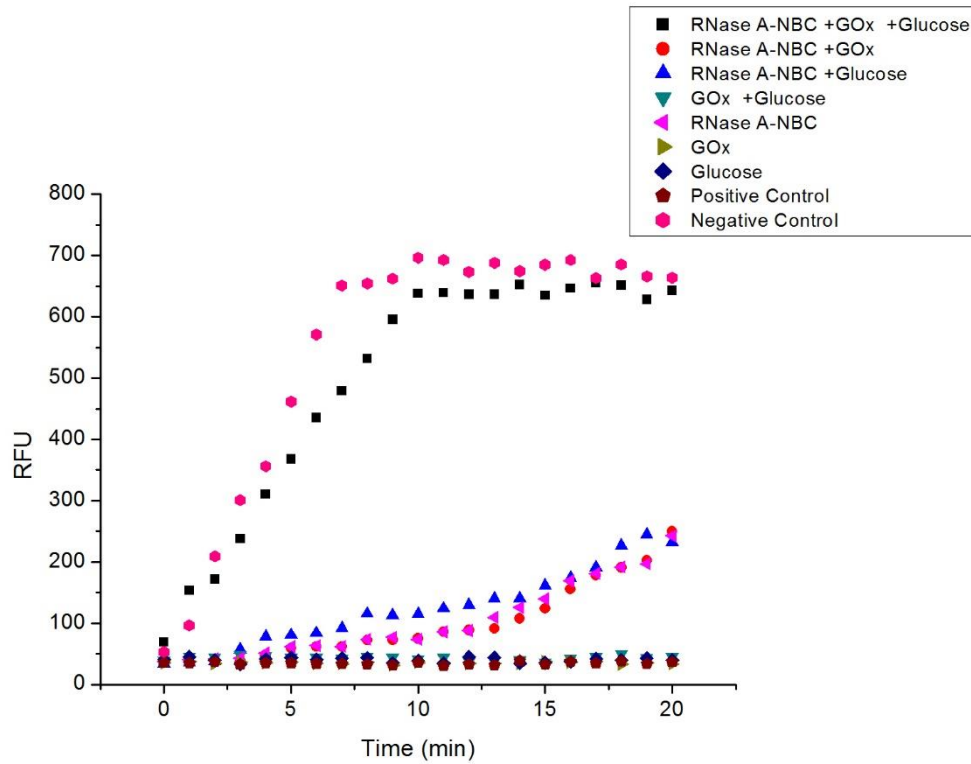


Figure 2.2 RNase A activity assay of RNase A-NBC with a variety of GOx and Glucose combinations. X-axis: Time of the reaction; Y-axis: relative fluorescence unit (RFU)

The result of RNase activity assay is summarized in **Figure 2.2**. The trajectories of relative fluorescence unit change, which indicates the change in reaction product and thus reflects RNase activity, are represented by dots with different shape. The curve for positive control is nearly horizontal around 0. However, the curve for negative control shows the most acute slope of increase during the assay. Together these two controls show the validity of this RNase A Activity Assay.

From the plot, the control groups of GOx only, glucose only, and GOx and glucose combination do not differ in their nuclease activity from the positive control. This means that none of glucose, GOx or GOx oxidized glucose has nuclease activity. In contrast, the control groups of RNase A-NBC only, RNase A-NBC and GOx combination, and RNase A-NBC and glucose combination all show weak nuclease activity. It is likely caused by the stock RNase A-NBC solution contains some amount of RNase A, since the RNase A-NBC is modified from RNase A by adding the NBC group.

The test group comprised of GOx, RNase A-NBC and glucose shows a similar assay curve with the negative control, suggesting the RNase activity of RNase A has been restored almost completely. Theoretically, this is triggered as GOx oxidizes glucose to gluconolactate and hydrogen peroxide, which in turn facilitate the self-immolative reaction of RNase A-NBC to destruct NBC protection, release lysine residual on RNase A and restore its activity.

In summary, as the preliminary study, the results of RNase A Activity Assay shows the feasibility to utilize the combined formulation of RNase A-NBC and GOx for the manipulation of RNase A activity under an environment containing glucose *in vitro*. To further investigate whether this system is able to function *in vivo* as well, RNase A-NBC and GOx were delivered by the cationic lipid-like nanoparticles EC16-80 into tumor cells to induce cytotoxic effects, as described in the following chapters.

CHAPTER 3. SYNERGISTIC EFFECT STUDY OF ROS-RESPONSIVE PROTEIN AND GOX DELIVERED BY THE CATIONIC LIPID-LIKE NANOPARTICLES

3.1 Materials and Methods

3.1.1 Materials

Unless otherwise noted, all cell culture reagents were purchased from Thermo Fisher Scientific (Waltham, MA), all vessels for cell culture were purchased from Corning (Corning, New York), and all other chemicals were purchased from Sigma-Aldrich (St. Louis, MO). The modified Protein, RNase A-NBC, was prepared by our Lab by method described in the previous report (Wang, Sun, et al. 2014).

3.1.2 Culture of HeLa Cells

HeLa cells were obtained from ATCC (Manassas, VA) and cultured in Dulbecco's Modified Eagle Medium (DMEM) with high glucose (4.5 g/L) supplemented with 10% (v/v) Fetal Bovine Serum (FBS) and 1% (v/v) Penicillin-Streptomycin (10,000 U/mL). Cell culture was maintained in T-75 flasks at 37°C in a 95% humidity and 5% CO₂ incubator. After reaching 70% - 80% confluence, cells were split at a ratio of 1: 3 by Trypsin-EDTA (0.25%).

3.1.3 *In Vitro* Cytotoxicity Assay Set-up

One day before delivery study, HeLa cells were removed from T-75 flasks and seeded in 96 well clear microplate at a concentration of 10,000 cells per well with 100 µL DMEM (high glucose).

3.1.4 Cytotoxicity Study of the Cationic Lipid-like Nanoparticles EC16-80 Dependent on the Concentration

A series of dilutions of EC16-80 ranging from 600 to 37.5 ng per well, by a factor of $\frac{1}{2}$, were prepared first. EC16-80 solution of each concentration was subsequently directly added to the 96 well plate set up. Cells without EC16-80 treatment were used as the negative control. After that, the plate was incubated at 37 °C for 24 h before cell viability measurement by MTT assay.

3.1.5 EC16-80/RNase A-NBC Nanoparticles Delivery

A series of dilutions of RNase-NBC ranging from 300 to 18.75 ng per well, by a factor of $\frac{1}{2}$, were prepared first. Then this series of RNase-NBC solutions were directly added to a 96 well plate set up. Cells without RNase A-NBC treatment were used as the negative control. After that, the plate was incubated at 37 °C for 24 h before cell viability measurement by MTT assay.

Another series of RNase A-NBC, with similar protein dilutions of concentration ranging from 300 to 18.75 ng per well, was mixed with 150 ng EC16-80 per well, followed by 15 min standing. Then this series of EC16-80/RNase A-NBC nanoparticles was added to another 96 well plate set up. Cells without EC16-80/RNase A-NBC treatment were used as the negative control. After that, the plate was incubated at 37 °C for 24 h before cell viability measurement by MTT assay.

3.1.6 EC16-80/GOx Nanoparticles Delivery

A series of dilutions of GOx ranging from 6 to 0.375 ng per well, by a factor of $\frac{1}{2}$, were prepared first. Subsequently this series of GOx solution was directly added to a 96 well plate set up. Cells without GOx treatment was used as the negative control. After that, the plate was incubated at 37 °C for 24 h before cell viability measurement by MTT assay.

The other series of dilutions of GOx ranging from 6 to 0.375 ng per well, by a factor of $\frac{1}{2}$, were prepared and mixed with 150 ng EC16-80 per well, followed by 15 min incubation. This series of EC16-80/GOx nanoparticles was then added to another 96 well plate set up. Cells without EC16-80/GOx treatment was used as the negative control. After that, the plate was incubated at 37 °C for 24 h before cell viability measurement by MTT assay.

3.1.7 Synergistic Effect of Protein Combination Delivery

The formulations were combination of GOx, RNase A-NBC and EC16-80 as **Table 3.1**. When preparing the formulations, reagents were mixed thoroughly and followed by 15 min standing. Then this series of nanoparticles was added to a 96 well plate set up. After that, the plate was incubated at 37 °C for 24 h before cell viability measurement by MTT assay.

Table 3.1 Combination Formulations of GOx, RNase A-NBC and EC16-80

Group	Treatment		
	Ec16-80 (ng)	RNase A-NBC (ng)	GOx (ng)
Control	0	0	0
1	0	0	1.5
2	0	75	0
3	0	75	1.5
4	150	0	0
5	150	0	1.5
6	150	75	0
7	150	75	1.5

3.1.8 Thiazolyl Blue Tetrazolium Bromide (MTT) Assay

The culture medium was used as solvent to prepare the 0.5 mg/mL MTT solution. MTT solution should be protected from light and stored no more than one day. After initializing protein delivery, the old medium was removed and replaced with 100 μ L per well warm (37 °C) MTT solution. A negative control should be included by adding 100 μ L per well MTT solution to blank wells. Cells were incubated at 37°C for one hour, and then the MTT solution was removed to stop the reaction. 100 μ L each well Dimethyl Sulfoxide (DMSO) solution was added and mixed with the pipette to ensure complete solubilization. The absorbance was read at 570 nm. An effective result of OD value should be no less than 0.4 and no greater than 1.4. After subtracting the background reading from empty wells, the cell viability was calculated by the ratio of treatment reading to control reading, as the following equation indicates:

$$Cell\ Viability = \frac{Treatment - Background}{Control - Background} \times 100\% \quad Eq. 3.1$$

3.2 Results and Discussion

3.2.1 Cytotoxicity of the Cationic Lipid-like Nanoparticles EC16-80 Dependent on the Protein Concentration

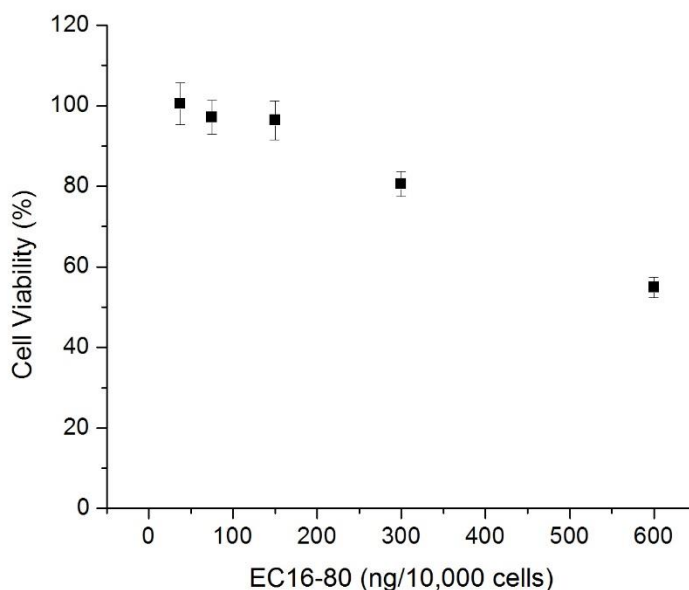


Figure 3.1 The cell viability assay to determine the cytotoxic concentration of EC16-80 lipidoid. The figures shows cell viability drops after the concentration increases above 150 ng per 10,000 cells while at low concentration the cell viability do not differ significantly.

Although the high concentration of cationic Lipid-like nanoparticles may increase the efficiency of protein delivery, lipidoids may themselves be cytotoxic to cells at high concentration. To obtain optimal balance between efficiency and non-toxicity, the cell viability curve was investigated to determine the upper bound of a non-toxic concentration of EC16-80. As shown in **Figure 3.1**, the HeLa cell viability varies with the change in EC16-80 concentration. At a low

level of EC16-80 treatment, ranging from 37.5 to 150 ng per 10,000 cells, the cell viability does not show a significant change. When the dose of EC16-80 is increased from 150 to 600 ng per 10,000 cells, the cell viability decreases from about 96.4% to about 54.9%. For the purpose of target delivery of cancer therapeutics, the concentration of EC16-80 should guarantee both the efficiency of protein delivery and nontoxicity to healthy cells. Therefore, the concentration of EC16-80 of 150 ng per 10,000 cells is considered as an appropriate dose for delivering the proposed GOx & RNase A – NBC system into HeLa cells model.

3.2.2 Cytotoxicity resulted from EC16-80/RNase A-NBC Nanoparticles Delivery

To confirm our assumption that RNase A-NBC itself cannot enter cell plasma, HeLa cells are next treated solely with RNase A-NBC, of which the dose goes from 18.75 to 300 ng per 10,000 cells. As Figure 3.2 shows, the cell viability does not significantly change with the increase of RNase A-NBC concentration. In other words, RNase A-NBC shows no cytotoxicity in the selected range, suggesting it cannot be transported transcellularly by itself.

To determine whether EC16-80 facilitates the transmembrane transport of RNase A-NBC, the cell viability assay was also conducted to determine whether increase in RNase A-NBC concentration associated with higher cytotoxicity at the presence of EC16-80. As Figure 3.3 shows, cytotoxicity of RNase A-NBC increases with higher RNase A-NBC level at the presence of EC16-80 with a dose of 150 ng per 10,000 cells. When treated with RNase A-NBC at 18.75 ng per 10,000 cells, the viability in HeLa cells are not significantly different from the control (100%

of cell viability in control). When the dose of the RNase A-NBC increases to 300 ng per 10,000 cells, around 75% HeLa cells are killed. This is consistent with our previous report and the hypothesis that the modified protein RNase A-NBC is reactivated inside HeLa cells by high levels of intracellular ROS, as RNase A cleaves RNA and induces cytotoxicity.

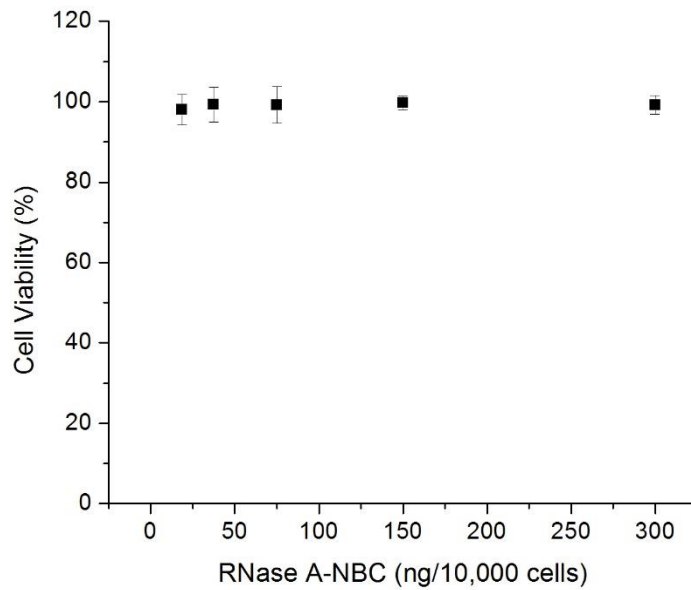


Figure 3.2 Cell viability assay to determine the association of RNase A – NBC concentration and cytotoxicity. The figure shows no significant change in cell viability with the variation in RNase A-NBC concentration.

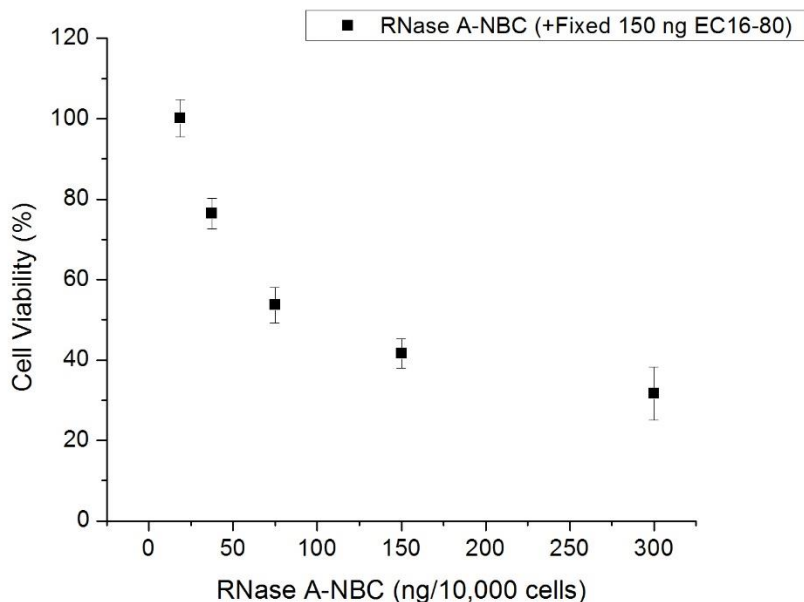


Figure 3.3 Cell viability assay to determine the association of RNase A – NBC concentration and cytotoxicity at the presence of EC16-80. The figure shows a sharp drop in cell viability with RNase A-NBC concentration increase within low concentration range, which flattens within high concentration range.

3.2.3 Cytotoxicity resulted from EC16-80/GOx Nanoparticles Delivery

In Figure 3.4 and Figure 3.5, GOx, either with or without the help of EC16-80, shows increasing cytotoxicity with its dose increasing at the presence of EC16-80 at 150ng per 10,000 cells. This is consistent with our hypothesis that GOx can oxidize either extracellular or intracellular glucose to gluconolactate and hydrogen peroxide, which in turn exhibits cytotoxicity when its dose reaches a certain amount. Interestingly, in both situations, the cell viability drops significantly, when the dose of GOx increases from 1.5 ng to 3 ng per 10,000 cells. At the lowest three dose tested (0, 0.75 and 1.5 ng /10,000 cells), viability does not differ significantly. In contrast, at the

highest two doses (3 and 6 ng /10,000 cells), the viability decrease with higher concentration but to a much smaller extent compared to the sharp drop occurs between 1.5 and 3 ng / 10,000 cells.

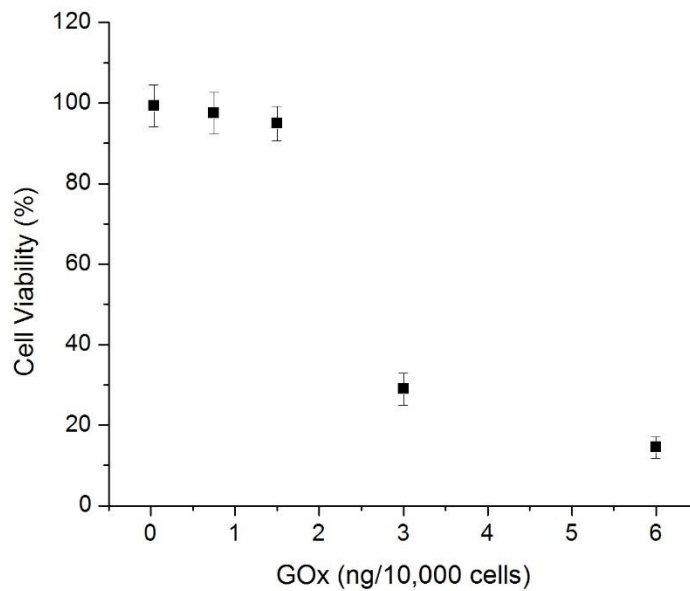


Figure 3.4 Cell viability assay to determine association of the cytotoxicity of GOx and its dose. The slope of change is much flatter at lower (<1.5 ng per 10,000 cells) and higher (>3 ng per 10,000 cells) concentration ranges compared to the sharp drop at the mid-range.

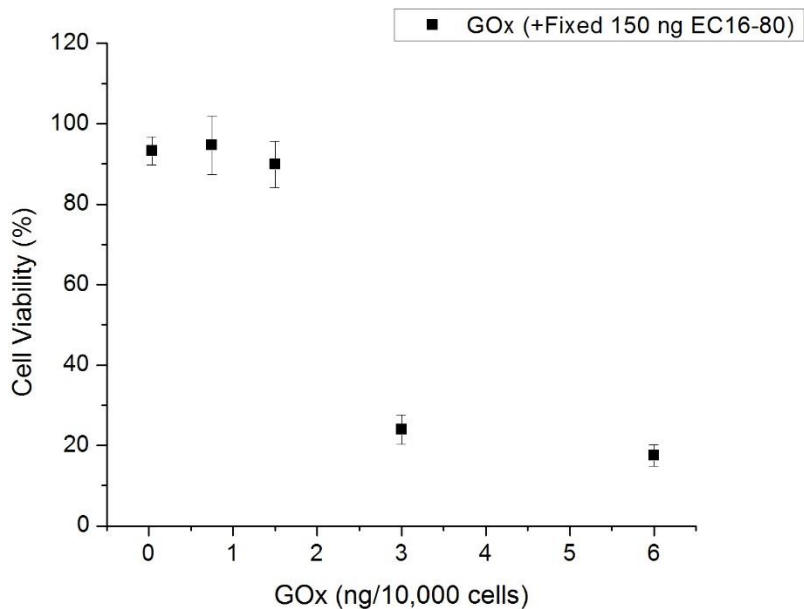


Figure 3.5 Cell viability assay to determine association of the cytotoxicity of GOx and its dose with the presence of EC16-80 at 150 ng / 10,000 cells. Similarly to what was observed after GOx only treatment, the cell viability sharply drop between 1.5 and 3 ng / 10,000 cells whereas remain constant at other concentrations.

3.2.4 Synergistic Effect of Protein Combination Delivery on HeLa cells

Since cytotoxic effects were observed in both RNase A-NBC with EC16-80 nanoparticles and GOx with/without EC16-80 nanoparticles, it is intriguing to know whether the combination of the RNase A-NBC and GOx, with the help of EC16-80 nanoparticles for intracellular delivery, can lead to greater efficacy on killing cancer cells, as known as producing the synergistic drug effect. Consistent with our expectation, as shown in Figure 3.6 the formulation of EC16-80 at 150 ng/ 10,000 cells, RNase A-NBC at 75 ng/ 10,000 cells and GOx at 1.5 ng/ 10,000 has the strongest ability to annihilate HeLa cells among all combinations tested. The cell death rate in this group

is approximately 60%, which is larger than the arithmetic sum of the death rate from the EC16-80 + GOx group (approximately 10%) and the EC16-80 + RNase A-NBC group (approximately 40%), clearly showing a synergistic effect.

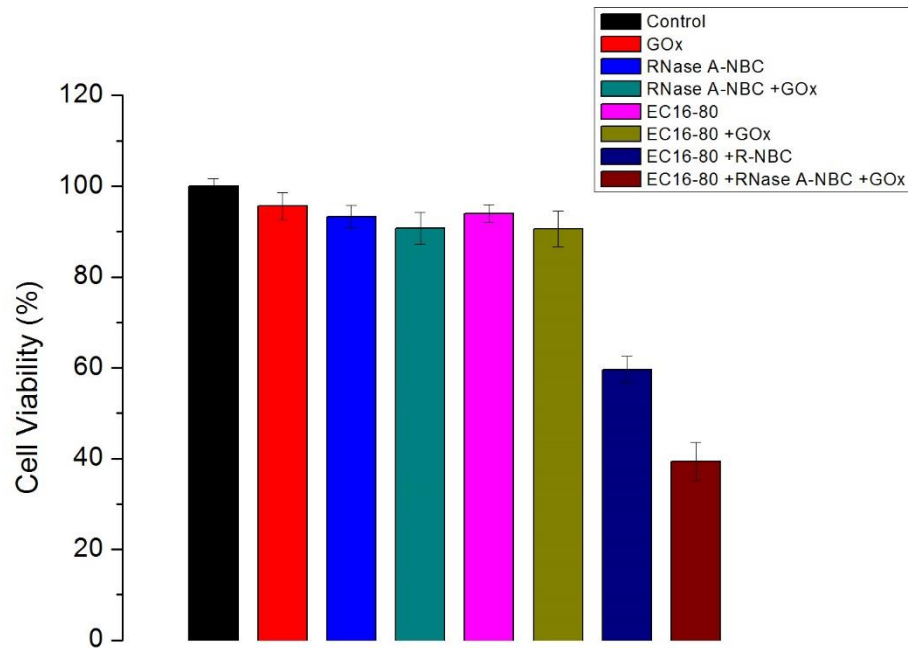


Figure 3.6 The viability of Hela cells across different drug delivery groups. The EC16-80 + RNase A-NBC + GOx group has the lowest viability and shows a synergistic effect on cell killing.

CHAPTER 4. STUDY OF GLUCOSE DEPENDENCE OF COMBINATION

FORMULATION

4.1 Materials and Methods

4.1.1 Materials

Unless otherwise noted, all cell culture reagents were purchased from Thermo Fisher Scientific (Waltham, MA), all vessels for cell culture were purchased from Corning (Durham, NC), and all chemicals were purchased from Sigma-Aldrich (St. Louis, MO). The modified Protein, RNase-NBC, was prepared by our lab using method described in previous report.

4.1.2 Increased Glucose Culture Treatment before Protein Combination Delivery

Double Glucose DMEM was prepared by adding 2.25 g glucose to per 500 mL DMEM (high glucose). One day before delivery experiment, HeLa cells were removed from T-75 flasks and seeded in 96 well clear microplate at a concentration of 10,000 cells per well with 100 μ L double glucose DMEM. The method of protein combination delivery was the same as reported in **Section 3.1.7**.

4.1.3 No Glucose Culture Treatment before Protein Combination Delivery

One day before delivery study, HeLa cells were detached from T-75 flasks and seeded in 96 well clear microplate at a concentration of 10,000 cells per well with 100 μ L DMEM without glucose. The method of protein combination delivery was the same as reported in **Section 3.1.7**.

4.1.4 Inhibition of GLUT Activity Treatment before Protein Combination Delivery

A 30 mg/mL stock phloretin solution was made by dissolving the phlorerin crystalline solid in DMSO. One day before delivery study, HeLa cells were detached from T-75 flasks and seeded in 96 well clear microplate at a concentration of 10,000 cells per well with 100 μ L DMEM plus 2.5 μ M phloretin for GLUT inhibition. The method of protein combination delivery was the same as reported in **Section 3.1.7**.

4.2 Results and Discussion

4.2.1 Results of Increased Glucose Culture Treatment for Protein Combination Delivery

To further confirm the synergistic effects between the GOx and RNase A-NBC, and investigate their dependency on glucose, HeLa cell was cultured in DMEM with doubled concentration of glucose before the drug delivery study on the next day. As shown in Figure 4.1, the double glucose treatment has some impacts on the viability pattern after drug delivery as the viability of HeLa cells are lower in the group GOx and the group EC16-80 + GOx, when compared to the control. This result is in discrepancy with Figure 3.6, in which these two combination groups

does not differ from the control. One possible explanation could be the higher level of hydrogen peroxide produced from glucose oxidation by GOx, since the media contains higher level of glucose. The extra hydrogen peroxide may reach certain threshold and trigger the cell destruction, and therefore lower their viability. The patterns for the group EC16-80 + RNase A-NBC and the group EC16-80 + RNase A-NBC +GOx are similar to that shown in Figure 3.6, suggesting extra glucose does not provide an additive effect on the RNase A-NBC's ability to kill HeLa cells.

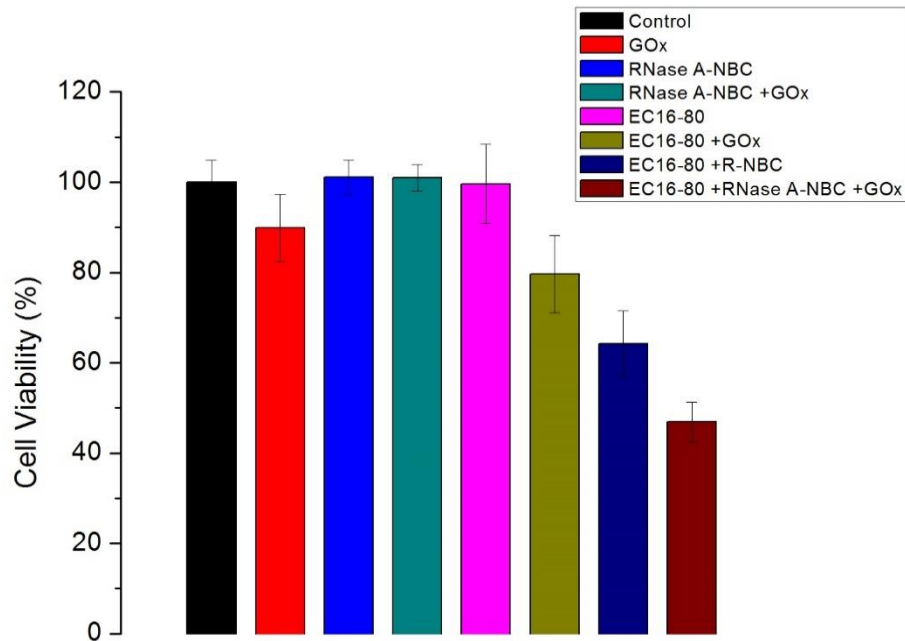


Figure 4.1 The viability of HeLa cells across different drug delivery groups, after double glucose culture for the day previous to study. The EC16-80 + RNase A-NBC + GOx group has the lowest viability. In the group GOx and the group EC16-80 + GOx, though with large variance, the viability are also lower than the control group.

4.2.2 Results of No Glucose Culture Treatment for Protein Combination Delivery

We also investigated the effects of glucose starvation on the GOx and RNase A-NBC combination. To achieve glucose starvation, HeLa cell was cultured in DMEM without glucose before the drug delivery study on the next day. As shown in figure 4.2, after glucose starvation the sensitivity of HeLa cells to RNase A-NBC and GOx was greatly reduced, in contrast to the observations represented by Figure 3.6 and Figure 4.1. This is consistent with our expectation as lacking of glucose to be oxidized by GOx would lead to the reduction in hydrogen peroxide generation, which in turn result in decreased rate of RNase A activity restoration. This result indicates that the combination formulations are glucose dependent.

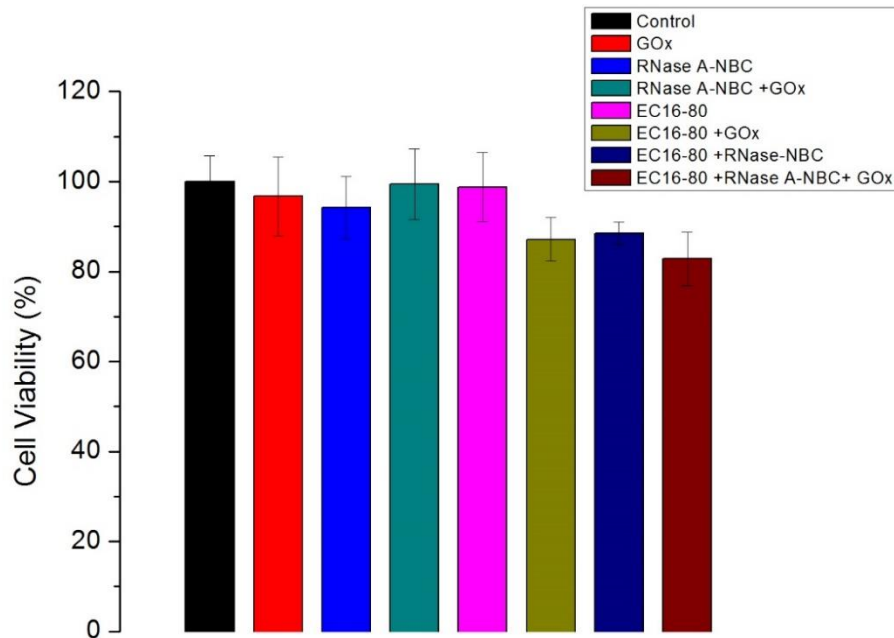


Figure 4.2 The viability of HeLa cells across different drug delivery groups, after glucose starvation for the day previous to study. Glucose deprivation greatly reduced the cytotoxic effect of GOx, RNase A-NBC or their combination.

4.2.3 Inhibition of GLUT Activity Treatment for Protein Combination Delivery

To further study the dependence of combination formulations on glucose, phloretin, which is a potent inhibitor for GLUT1 and GLUT2, was examined for its effects on the combination formulation. As shown in Figure 4.3, with phloretin, the cell viability for the group EC16-80 + RNase A-NBC and the group EC16-80 + RNase A-NBC + GOx are approximately 80% and 60%, higher than their counterparts in normal culture condition (approximately 60% and 40%) (Figure 3.6). This demonstrates that the inhibition of GLUT decreases the cytotoxic effect of RNase A-NBC and GOx for HeLa cells and supports that the combination formulations are dependent on glucose.

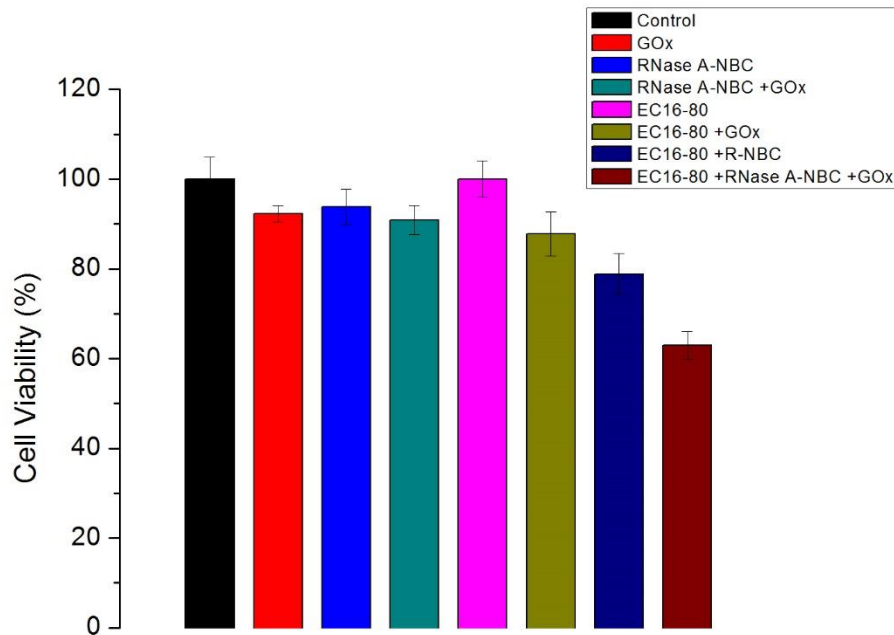


Figure 4.3 The viability of HeLa cells across different drug delivery groups, after phloretin treatment to inhibit the GLUTs and thus the intracellular transport of glucose. The result shows inhibition of GLUTs reduced the cytotoxic effect of GOx, RNase A-NBC or their combination.

CHAPTER 5. CONCLUSIONS

As demonstrated previously in our lab, the RNase A-NBC carried by lipidoid nanoparticle EC16-80 can be successfully delivered into and kill cancer cells whereas leave normal cell untouched. This indicates a promising prospect for the application of lipidoid nanoparticle onto treatment of cancers.

In this project, by taking advantage of the mechanism of RNase A-NBC modification and restoration, we improved the efficacy of RNase A-NBC delivery on killing cancer cells by combining it with GOx delivery. We successfully demonstrated the combination formulation of RNase A-NBC and GOx, when taken up together into tumor cells, has a synergistic effect of cytotoxicity stronger than EC16-80 delivered RNase A-NBC or GOx alone. The result shown in the paper supports our expectation that RNase A-NBC can be reactivated inside tumor cells by hydrogen peroxide generated by GOx, and accordingly restore the cytotoxicity of RNase A.

In this paper, we also demonstrated that the above process is glucose dependent by cell viability assays. As tumor cells have higher cellular glucose concentration than normal cells, the glucose dependency gives the combination formulation specific cytotoxicity against tumor cells. At the same time, it would remain safe for normal cells. From my point of view, the combination formulation of RNase A-NBC and GOx has huge potential for targeted cancer therapies and brilliant future of application.

REFERENCE

1. Achilli, C., A. Ciana, M. Fagnoni, C. Balduini, and G. Minetti. 2013. "Susceptibility to hydrolysis of phenylboronic pinacol esters at physiological pH." *Central European Journal of Chemistry* 11 (2):137-139. doi: DOI 10.2478/s11532-012-0159-2.
2. Adekola, K., S. T. Rosen, and M. Shanmugam. 2012. "Glucose transporters in cancer metabolism." *Curr Opin Oncol* 24 (6):650-4. doi: 10.1097/CCO.0b013e328356da72.
3. Afzal, I., P. Cunningham, and R. J. Naftalin. 2002. "Interactions of ATP, oestradiol, genistein and the anti-oestrogens, faslodex (ICI 182780) and tamoxifen, with the human erythrocyte glucose transporter, GLUT1." *Biochem J* 365 (Pt 3):707-19. doi: 10.1042/BJ20011624.
4. Akinc, A., A. Zumbuehl, M. Goldberg, E. S. Leshchiner, V. Busini, N. Hossain, S. A. Bacallado, D. N. Nguyen, J. Fuller, R. Alvarez, A. Borodovsky, T. Borland, R. Constien, A. de Fougères, J. R. Dorkin, K. Narayanannair Jayaprakash, M. Jayaraman, M. John, V. Koteliansky, M. Manoharan, L. Nechev, J. Qin, T. Racie, D. Raitcheva, K. G. Rajeev, D. W. Sah, J. Soutschek, I. Toudjarska, H. P. Vornlocher, T. S. Zimmermann, R. Langer, and D. G. Anderson. 2008. "A combinatorial library of lipid-like materials for delivery of RNAi therapeutics." *Nat Biotechnol* 26 (5):561-9. doi: 10.1038/nbt1402.
5. Alabi, C. A., K. T. Love, G. Sahay, H. Yin, K. M. Luly, R. Langer, and D. G. Anderson. 2013. "Multiparametric approach for the evaluation of lipid nanoparticles for siRNA delivery." *Proc Natl Acad Sci U S A* 110 (32):12881-6. doi: 10.1073/pnas.1306529110.

6. Anand, P., A. B. Kunnumakkara, C. Sundaram, K. B. Harikumar, S. T. Tharakan, O. S. Lai, B. Sung, and B. B. Aggarwal. 2008. "Cancer is a preventable disease that requires major lifestyle changes." *Pharm Res* 25 (9):2097-116. doi: 10.1007/s11095-008-9661-9.
7. Annibaldi, A., and C. Widmann. 2010. "Glucose metabolism in cancer cells." *Curr Opin Clin Nutr Metab Care* 13 (4):466-70. doi: 10.1097/MCO.0b013e32833a5577.
8. Ardelt, W., S. M. Mikulski, and K. Shogen. 1991. "Amino acid sequence of an anti-tumor protein from *Rana pipiens* oocytes and early embryos. Homology to pancreatic ribonucleases." *J Biol Chem* 266 (1):245-51.
9. Augustin, R. 2010. "The protein family of glucose transport facilitators: It's not only about glucose after all." *IUBMB Life* 62 (5):315-33. doi: 10.1002/iub.315.
10. Azad, N., Y. Rojanasakul, and V. Vallyathan. 2008. "Inflammation and lung cancer: roles of reactive oxygen/nitrogen species." *J Toxicol Environ Health B Crit Rev* 11 (1):1-15. doi: 10.1080/10937400701436460.
11. Bao, J., K. Furumoto, M. Yoshimoto, K. Fukunaga, and K. Nakao. 2003. "Competitive inhibition by hydrogen peroxide produced in glucose oxidation catalyzed by glucose oxidase." *Biochemical Engineering Journal* 13 (1):69-72. doi: Pii S1369-703x(02)00120-1
Doi 10.1016/S1369-703x(02)00120-1.
12. Boveris, A., and B. Chance. 1973. "The mitochondrial generation of hydrogen peroxide. General properties and effect of hyperbaric oxygen." *Biochem J* 134 (3):707-16.

13. Broaders, K. E., S. Grandhe, and J. M. Frechet. 2011. "A biocompatible oxidation-triggered carrier polymer with potential in therapeutics." *J Am Chem Soc* 133 (4):756-8. doi: 10.1021/ja110468v.
14. Chan, D. A., P. D. Sutphin, P. Nguyen, S. Turcotte, E. W. Lai, A. Banh, G. E. Reynolds, J. T. Chi, J. Wu, D. E. Solow-Cordero, M. Bonnet, J. U. Flanagan, D. M. Bouley, E. E. Graves, W. A. Denny, M. P. Hay, and A. J. Giaccia. 2011. "Targeting GLUT1 and the Warburg effect in renal cell carcinoma by chemical synthetic lethality." *Sci Transl Med* 3 (94):94ra70. doi: 10.1126/scitranslmed.3002394.
15. Chan, S. S., and W. D. Lotspeich. 1962. "Comparative effects of phlorizin and phloretin on glucose transport in the cat kidney." *Am J Physiol* 203:975-9.
16. Copeland, W. C., J. T. Wachsman, F. M. Johnson, and J. S. Penta. 2002. "Mitochondrial DNA alterations in cancer." *Cancer Invest* 20 (4):557-69.
17. Croce, C. M. 2008. "Oncogenes and cancer." *N Engl J Med* 358 (5):502-11. doi: 10.1056/NEJMra072367.
18. de Gracia Lux, C., S. Joshi-Barr, T. Nguyen, E. Mahmoud, E. Schopf, N. Fomina, and A. Almutairi. 2012. "Biocompatible polymeric nanoparticles degrade and release cargo in response to biologically relevant levels of hydrogen peroxide." *J Am Chem Soc* 134 (38):15758-64. doi: 10.1021/ja303372u.
19. Fridovich, I. 1995. "Superoxide radical and superoxide dismutases." *Annu Rev Biochem* 64:97-112. doi: 10.1146/annurev.bi.64.070195.000525.

20. Ghosh, P., X. C. Yang, R. Arvizo, Z. J. Zhu, S. S. Agasti, Z. H. Mo, and V. M. Rotello. 2010. "Intracellular Delivery of a Membrane-Impermeable Enzyme in Active Form Using Functionalized Gold Nanoparticles." *Journal of the American Chemical Society* 132 (8):2642-2645. doi: DOI 10.1021/ja907887z.
21. Grabellus, F., J. Nagarajah, A. Bockisch, K. W. Schmid, and S. Y. Sheu. 2012. "Glucose transporter 1 expression, tumor proliferation, and iodine/glucose uptake in thyroid cancer with emphasis on poorly differentiated thyroid carcinoma." *Clin Nucl Med* 37 (2):121-7. doi: 10.1097/RLU.0b013e3182393599.
22. Hanahan, D., and R. A. Weinberg. 2011. "Hallmarks of cancer: the next generation." *Cell* 144 (5):646-74. doi: 10.1016/j.cell.2011.02.013.
23. Hlavata, L., H. Aguilaniu, A. Pichova, and T. Nystrom. 2003. "The oncogenic RAS2(val19) mutation locks respiration, independently of PKA, in a mode prone to generate ROS." *EMBO J* 22 (13):3337-45. doi: 10.1093/emboj/cdg314.
24. Joost, H. G., and B. Thorens. 2001. "The extended GLUT-family of sugar/polyol transport facilitators: nomenclature, sequence characteristics, and potential function of its novel members (review)." *Mol Membr Biol* 18 (4):247-56.
25. Jun, Y. J., S. M. Jang, H. L. Han, K. H. Lee, K. S. Jang, and S. S. Paik. 2011. "Clinicopathologic significance of GLUT1 expression and its correlation with Apaf-1 in colorectal adenocarcinomas." *World J Gastroenterol* 17 (14):1866-73. doi: 10.3748/wjg.v17.i14.1866.

26. Kang, D., and N. Hamasaki. 2003. "Mitochondrial oxidative stress and mitochondrial DNA." *Clin Chem Lab Med* 41 (10):1281-8. doi: 10.1515/CCLM.2003.195.
27. Kim, S. K., M. B. Foote, and L. Huang. 2012. "The targeted intracellular delivery of cytochrome C protein to tumors using lipid-apolipoprotein nanoparticles." *Biomaterials* 33 (15):3959-3966. doi: DOI 10.1016/j.biomaterials.2012.02.010.
28. Kleppe, K. 1966. "The effect of hydrogen peroxide on glucose oxidase from *Aspergillus niger*." *Biochemistry* 5 (1):139-43.
29. Kobori, M., H. Shinmoto, T. Tsushida, and K. Shinohara. 1997. "Phloretin-induced apoptosis in B16 melanoma 4A5 cells by inhibition of glucose transmembrane transport." *Cancer Lett* 119 (2):207-12.
30. Krupka, R. M. 1985. "Asymmetrical binding of phloretin to the glucose transport system of human erythrocytes." *J Membr Biol* 83 (1-2):71-80.
31. Leader, B., Q. J. Baca, and D. E. Golan. 2008. "Protein therapeutics: a summary and pharmacological classification." *Nat Rev Drug Discov* 7 (1):21-39. doi: 10.1038/nrd2399.
32. Lee, J. E., and R. T. Raines. 2008. "Ribonucleases as novel chemotherapeutics - The ranpirnase example." *Biodrugs* 22 (1):53-58.
33. Lee, J. S., and J. Feijen. 2012. "Polymersomes for drug delivery: Design, formation and characterization." *Journal of Controlled Release* 161 (2):473-483. doi: DOI 10.1016/j.jconrel.2011.10.005.

34. Leland, P. A., L. W. Schultz, B. M. Kim, and R. T. Raines. 1998. "Ribonuclease A variants with potent cytotoxic activity." *Proc Natl Acad Sci U S A* 95 (18):10407-12.
35. Leskovac, V., S. Trivic, G. Wohlfahrt, J. Kandrak, and D. Pericin. 2005. "Glucose oxidase from *Aspergillus niger*: the mechanism of action with molecular oxygen, quinones, and one-electron acceptors." *International Journal of Biochemistry & Cell Biology* 37 (4):731-750. doi: DOI 10.1016/j.biocel.2004.10.014.
36. Macheda, M. L., S. Rogers, and J. D. Best. 2005. "Molecular and cellular regulation of glucose transporter (GLUT) proteins in cancer." *J Cell Physiol* 202 (3):654-62. doi: 10.1002/jcp.20166.
37. Marshall, G. R., J. A. Feng, and D. J. Kuster. 2008. "Back to the future: ribonuclease A." *Biopolymers* 90 (3):259-77. doi: 10.1002/bip.20845.
38. McBrayer, S. K., J. C. Cheng, S. Singhal, N. L. Krett, S. T. Rosen, and M. Shanmugam. 2012. "Multiple myeloma exhibits novel dependence on GLUT4, GLUT8, and GLUT11: implications for glucose transporter-directed therapy." *Blood* 119 (20):4686-97. doi: 10.1182/blood-2011-09-377846.
39. Medina, R. A., and G. I. Owen. 2002. "Glucose transporters: expression, regulation and cancer." *Biol Res* 35 (1):9-26.
40. Medina Villaamil, V., G. Aparicio Gallego, L. Valbuena Rubira, R. Garcia Campelo, M. Valladares-Ayerbes, E. Grande Pulido, M. Victoria Bolos, I. Santamarina Cainzos, and L. M.

Anton Aparicio. 2011. "Fructose transporter GLUT5 expression in clear renal cell carcinoma." *Oncol Rep* 25 (2):315-23. doi: 10.3892/or.2010.1096.

41. Merrifield, B. 1985. "Solid-Phase Synthesis." *Bioscience Reports* 5 (5):353-376. doi: Doi 10.1007/Bf01116553.

42. Mi, Z., J. Mai, X. Lu, and P. D. Robbins. 2000. "Characterization of a class of cationic peptides able to facilitate efficient protein transduction in vitro and in vivo." *Mol Ther* 2 (4):339-47. doi: 10.1006/mthe.2000.0137.

43. Miron, J., M. P. Gonzalez, J. A. Vazquez, L. Pastrana, and M. A. Murado. 2004. "A mathematical model for glucose oxidase kinetics, including inhibitory, deactivant and diffusional effects, and their interactions." *Enzyme and Microbial Technology* 34 (5):513-522. doi: DOI 10.1016/j.enzmictec.2003.12.003.

44. Nelson, J. A., and R. E. Falk. 1993. "The efficacy of phloridzin and phloretin on tumor cell growth." *Anticancer Res* 13 (6A):2287-92.

45. Pazur, J. H., and K. Kleppe. 1964. "Oxidation of Glucose + Related Compounds by Glucose Oxidase from *Aspergillus Niger*." *Biochemistry* 3 (4):578-&. doi: DOI 10.1021/bi00892a018.

46. Pelicano, H., D. Carney, and P. Huang. 2004. "ROS stress in cancer cells and therapeutic implications." *Drug Resist Updat* 7 (2):97-110. doi: 10.1016/j.drug.2004.01.004.

47. Plummer, T. H., and C. H. W. Hirs. 1963. "Isolation of Ribonuclease B, a Glycoprotein, from Bovine Pancreatic Juice." *Journal of Biological Chemistry* 238 (4):1396-&.

48. Raines, R. T. 1998. "Ribonuclease A." *Chemical Reviews* 98 (3):1045-1065. doi: DOI 10.1021/cr960427h.
49. Reinicke, K., P. Sotomayor, P. Cisterna, C. Delgado, F. Nualart, and A. Godoy. 2012. "Cellular distribution of Glut-1 and Glut-5 in benign and malignant human prostate tissue." *J Cell Biochem* 113 (2):553-62. doi: 10.1002/jcb.23379.
50. Rodriguez-Enriquez, S., A. Marin-Hernandez, J. C. Gallardo-Perez, and R. Moreno-Sanchez. 2009. "Kinetics of transport and phosphorylation of glucose in cancer cells." *J Cell Physiol* 221 (3):552-9. doi: 10.1002/jcp.21885.
51. Saxena, S. K., S. M. Rybak, G. Winkler, H. M. Meade, P. Mcgray, R. J. Youle, and E. J. Ackerman. 1991. "Comparison of Rnases and Toxins Upon Injection into Xenopus Oocytes." *Journal of Biological Chemistry* 266 (31):21208-21214.
52. Saybasili, H., M. Yuksel, G. Haklar, and A. S. Yalcin. 2001. "Effect of mitochondrial electron transport chain inhibitors on superoxide radical generation in rat hippocampal and striatal slices." *Antioxid Redox Signal* 3 (6):1099-104. doi: 10.1089/152308601317203602.
53. Shim, M. S., and Y. Xia. 2013. "A reactive oxygen species (ROS)-responsive polymer for safe, efficient, and targeted gene delivery in cancer cells." *Angew Chem Int Ed Engl* 52 (27):6926-9. doi: 10.1002/anie.201209633.
54. Staniek, K., L. Gille, A. V. Kozlov, and H. Nohl. 2002. "Mitochondrial superoxide radical formation is controlled by electron bifurcation to the high and low potential pathways." *Free Radical Research* 36 (4):381-387. doi: Doi 10.1080/10715760290021225.

55. Sun, S., M. Wang, S. A. Knupp, Y. Soto-Feliciano, X. Hu, D. L. Kaplan, R. Langer, D. G. Anderson, and Q. Xu. 2012. "Combinatorial library of lipidoids for in vitro DNA delivery." *Bioconjug Chem* 23 (1):135-40. doi: 10.1021/bc200572w.
56. Torchilin, V. 2009. "Intracellular delivery of protein and peptide therapeutics." *Drug Discovery Today: Technologies* 5 (2-3):e95-e103.
57. Vafa, O., M. Wade, S. Kern, M. Beeche, T. K. Pandita, G. M. Hampton, and G. M. Wahl. 2002. "c-Myc can induce DNA damage, increase reactive oxygen species, and mitigate p53 function: a mechanism for oncogene-induced genetic instability." *Mol Cell* 9 (5):1031-44.
58. Van Driel, B. E., H. Lyon, D. C. Hoogenraad, S. Anten, U. Hansen, and C. J. Van Noorden. 1997. "Expression of CuZn- and Mn-superoxide dismutase in human colorectal neoplasms." *Free Radic Biol Med* 23 (3):435-44.
59. Vander Heiden, M. G., L. C. Cantley, and C. B. Thompson. 2009. "Understanding the Warburg effect: the metabolic requirements of cell proliferation." *Science* 324 (5930):1029-33. doi: 10.1126/science.1160809.
60. Vera, J. C., A. M. Reyes, J. G. Carcamo, F. V. Velasquez, C. I. Rivas, R. H. Zhang, P. Strobel, R. Iribarren, H. I. Scher, J. C. Slebe, and et al. 1996. "Genistein is a natural inhibitor of hexose and dehydroascorbic acid transport through the glucose transporter, GLUT1." *J Biol Chem* 271 (15):8719-24.

61. Walker, J., H. B. Jijon, H. Diaz, P. Salehi, T. Churchill, and K. L. Madsen. 2005. "5-aminoimidazole-4-carboxamide riboside (AICAR) enhances GLUT2-dependent jejunal glucose transport: a possible role for AMPK." *Biochem J* 385 (Pt 2):485-91. doi: 10.1042/BJ20040694.
62. Wang, M., K. Alberti, S. Sun, C. L. Arellano, and Q. Xu. 2014. "Combinatorially designed lipid-like nanoparticles for intracellular delivery of cytotoxic protein for cancer therapy." *Angew Chem Int Ed Engl* 53 (11):2893-8. doi: 10.1002/anie.201311245.
63. Wang, M., S. Sun, K. A. Alberti, and Q. Xu. 2012. "A combinatorial library of unsaturated lipidoids for efficient intracellular gene delivery." *ACS Synth Biol* 1 (9):403-7. doi: 10.1021/sb300023h.
64. Wang, M., S. Sun, C. I. Neufeld, B. Perez-Ramirez, and Q. Xu. 2014. "Reactive oxygen species-responsive protein modification and its intracellular delivery for targeted cancer therapy." *Angew Chem Int Ed Engl* 53 (49):13444-8. doi: 10.1002/anie.201407234.
65. Warburg, O. 1956. "On the origin of cancer cells." *Science* 123 (3191):309-14.
66. Wilson, R., and A. P. F. Turner. 1992. "Glucose-Oxidase - an Ideal Enzyme." *Biosensors & Bioelectronics* 7 (3):165-185. doi: Doi 10.1016/0956-5663(92)87013-F.
67. Wong, C. M., K. H. Wong, and X. D. Chen. 2008. "Glucose oxidase: natural occurrence, function, properties and industrial applications." *Appl Microbiol Biotechnol* 78 (6):927-38. doi: 10.1007/s00253-008-1407-4.

68. Wood, T. E., S. Dalili, C. D. Simpson, R. Hurren, X. Mao, F. S. Saiz, M. Gronda, Y. Eberhard, M. D. Minden, P. J. Bilan, A. Klip, R. A. Batey, and A. D. Schimmer. 2008. "A novel inhibitor of glucose uptake sensitizes cells to FAS-induced cell death." *Mol Cancer Ther* 7 (11):3546-55. doi: 10.1158/1535-7163.MCT-08-0569.
69. Wuest, M., B. J. Trayner, T. N. Grant, H. S. Jans, J. R. Mercer, D. Murray, F. G. West, A. J. McEwan, F. Wuest, and C. I. Cheeseman. 2011. "Radiopharmacological evaluation of 6-deoxy-6-[¹⁸F]fluoro-D-fructose as a radiotracer for PET imaging of GLUT5 in breast cancer." *Nucl Med Biol* 38 (4):461-75. doi: 10.1016/j.nucmedbio.2010.11.004.